energies

MDPI

Article

Wind Power Ramps Driven by Windstorms and Cyclones

Madalena Lacerda *, António Couto and Ana Estanqueiro

Unidade de Energias Renováveis e Integração de Sistemas de Energia, Laboratório Nacional de Energia e Geologia, I.P. (LNEG), 1649-038 Lisbon, Portugal; antonio.couto@lneg.pt (A.C.); ana.estanqueiro@lneg.pt (A.E.)
* Correspondence: madalena.lacerda@lneg.pt

Received: 16 August 2017; Accepted: 20 September 2017; Published: 23 September 2017

Abstract: The increase in the wind power predictability assumes a very important role for secure power system operation at minimum costs, especially in situations with severe changes in wind power production. In order to improve the forecast of such events, also known as "wind power ramp events", the underlying role of some severe meteorological phenomena in triggering wind power ramps must be clearly understood. In this paper, windstorm and cyclone detection algorithms are implemented using historical reanalysis data allowing the identification of key characteristics (e.g., location, intensity and trajectories) of the events with the highest impact on the wind power ramp events in Portugal. The results show a strong association between cyclones/windstorms and wind power ramp events. Moreover, the results highlight that it is possible to use some features of these meteorological phenomena to detect, in an early stage, severe wind power ramps thus creating the possibility to develop operational decision tools in order to support the security of power systems with high amounts of wind power generation.

Keywords: wind power ramps; cyclonic activity; power generation system management; weather conditions; windstorms

1. Introduction

The strong investment in renewable energy sources with a stochastic behavior, such as wind power, has brought new challenges to transmission system operators (TSOs) [1,2]. Thus, in the current context of large-scale integration in countries like Portugal, where wind power production represents 24% of the annual electricity consumption [3], increasing its predictability assumes a crucial role in order to guarantee a secure and cost-effective management of the consumption/ production binomial [4,5].

Currently, for the efficient and safe operation of a power system [4,5], a reliable wind power production forecast is required, that when coupled with a load forecast system, enables a reduction in the need to balance the energy on the reserve markets, at high costs [6]. Despite the fact that most TSOs currently use wind power forecast systems, these still face substantial errors (in phase and magnitude), especially during periods with severe variations in the wind power production [7]. These errors occur, in most cases, due to the inability of current forecast techniques to deal with the sudden dynamical structures observed in the atmospheric circulation [7] that in turn trigger rapid changes in the power production.

Recent studies strive to understand these dynamics, for instance, [4] states that holistic methodologies capable of comprising the spatiotemporal evolution of atmospheric large-scale circulation are needed in order to enhance and complement the current forecasting techniques. These results are also supported by other authors, who associate atmospheric phenomena (e.g., cold fronts and troughs) [4,8] as the critical weather situations for the TSO, namely to maintain the

balance between production and consumption in order to ensure the stability of the power system, especially during the so-called "wind power ramp events" [9]. In fact, in [8] the authors suggest an automated cyclone detection algorithm for recognition of critical weather situations for wind power integration. As stated by [10], cyclonic events are not always accompanied by strong winds, which is the primary wind power resource. Consequently, this study focuses on the application of windstorm [10] and cyclone [11] detection algorithms aiming to understand the basis of large-scale meteorological mechanisms capable of unleashing severe wind power ramps in the Portuguese national aggregate. Thus, this work contributes to: (i) a better understanding of the main meteorological features behind the wind power ramp events, and (ii) assessing the capabilities of windstorm/cyclone detection algorithms [10,11] to identify wind power ramps as well as their main impacts on the wind power production. Understanding the role of such phenomena will allow to: (i) minimize the impact of large-scale wind power integration within a power system; and (ii) develop reliable operational diagnostic tools for wind power ramps [5,12,13] that can be easily integrated into the decision making process by a TSO [5].

In Section 2, a detailed literature review regarding the relationship between weather phenomena and wind power production is presented. Section 3 describes the methodologies applied for windstorm and cyclone detection as well as the definitions used for the wind power ramp detection algorithm. Section 4 presents and discusses the link between cyclones/windstorms and wind power ramp events in Portugal along with the impact level of such weather situations. Within this section, a cluster analysis was applied to identify windstorm/cyclone trajectories with the most influence on the wind power production in Portugal. Finally, in Section 5 some conclusions are drawn.

2. Weather and Wind Power Ramps

The role of atmospheric circulation in triggering wind power ramps is a relatively new research topic, however, there has been a significant increase in the number of published studies and projects on this topic and on the adjacent causes behind the occurrence of wind power ramps [14]. Understanding such events is not an easy task as the weather conditions are rarely the same for different wind parks. In fact, even when two wind parks are located in similar latitudes, local effects may differ due to the terrain characteristics, roughness and topography or even due to phenomena like sea/land breezes [14]. Moreover, also the layout of the wind park, as well as its size, can (or not) justify the occurrence of wind power ramps through meteorological processes involving changes in wind direction [14]. Additionally, it is well documented that aggregating wind parks with a wide geographical dispersion enables one to take advantage of the lack of spatiotemporal correlation of the wind resource. This is one of the most basic features for wind resources, which can nullify, in some cases, the rapid fluctuations of wind power production. In the literature, this effect is entitled statistical power smoothing [4], and can be extremely beneficial to the operation and management of the power system.

Notwithstanding this, several authors [4,14,15] have indicated that the aggregation of wind parks, even when widely dispersed, is not enough to mitigate some events, especially when an entire country (or a control zone) is immersed under certain weather conditions with a coherent structure, which usually extends over several hundreds of kilometers (e.g., cold fronts). Indeed, in [14] the authors identified areas of strong convection, fronts and low-level jets as the major drivers for wind power ramp events. Using a classification of the weather situations, in [16] the authors concluded that the greatest impact on the wind power production is expected during: (i) large-scale weather systems, such as cold fronts; and (ii) local/mesoscale circulations, namely sea/land breezes and mountain/valley breezes. In [17], this topic was also addressed, in particular, the distinction between meteorological processes often responsible for the occurrence of upward-ramp events (e.g., cold fronts, thunderstorms, mountain/sea breezes) and downward-ramp events (e.g., relaxation after the passage of a cold front and warm front). Furthermore, the author showed that downward-ramp events are less frequent than upward-ramps. According to the authors, this may be explained by the passage of weather systems, such as cold fronts, causing a sudden increase in wind speed followed by a gradual

decrease. Reference [18] also found that the upward-ramps are mainly caused by convective events during warm seasons (spring and summer) and the passage of frontal systems during cold seasons (autumn and winter). Reference [19] compared the causes under the occurrence of 154 wind power ramps in a wind park in Pomeroy (IA, USA) with 1485 wind power ramp events from six wind turbines in a wind park in Iowa, about 160 km away, for the same time period. The authors found that 40% of the ramps that took place in the wind park in Iowa, occurred within a time interval of 6 h from a ramp detected in Pomeroy, suggesting some spatial consistency regarding the occurrence of wind power ramps. The same authors also reported that 20% of the ramps that occurred simultaneously in central Iowa and Pomeroy were due to the passage of large-scale systems with strong pressure gradients. Through visual inspection, in [12] the author identified the weather situations with the greatest influence in wind power production. In fact, using data from three wind parks, the author found that 40% of the large and rapid variations in wind power production were caused by the passage of cold fronts near the parks' locations. Low pressure systems account for 15% of these sudden changes, while the category "between systems" covers about 25% of the cases. These results highlight the relationship between wind power ramps and large-scale weather systems. Using computer vision techniques, in [20] an innovative approach for the determination of low pressure valleys associated with wind power ramps was developed. The authors found that, in fact, the geometry of low pressure valleys can successfully distinguish situations with the occurrence of wind power ramps from the ones without. Regarding the Portuguese case, in [4] through a manual and automatic identification, the authors concluded that strong wind power ramp events are usually detected during the winter. During this period, upward-ramp events are mostly associated with low pressure systems and fronts on the North/Centre regions of Portugal, while downward-ramp events are normally generated by a decrease in speed caused by the passage of low pressure centers with a direction towards the mainland. During the summer, both the frequency and the intensity of the events are reduced resulting, in many cases, in the intensification of the thermal low pressure system over the Iberian Peninsula [4]. These results indicate that for the Portuguese national aggregate production the following conditions apply: (i) seasonality has a high impact on wind power production; and (ii) the synoptic structures identified during the winter extend over large areas and have a characteristic signature. Most recently, in [8] the authors showed that high wind power forecast errors in the day-ahead market are linked to special weather patterns. Indeed, in this work it was possible to conclude that in 60.2% of the days with the most impactful wind power forecast errors, a cyclone or a trough moved over the North Sea, the Baltic Sea or directly over Germany. The authors also constructed an automated critical weather tool for Germany based on a cyclone detection algorithm aiming to support the integration of wind power in the day-ahead electricity market. This is an example of the applicability of weather dependent tools that can be easily incorporated in the decision making process of the TSO.

3. Data and Methodology

In this section, both the data used and methodologies applied for cyclone/windstorm detection are addressed. In this work, a circulation-to-environment approach was followed [21], which is usually performed in two steps. First, the meteorological systems (cyclones or windstorms) are identified based on the selected meteorological variables (circulation variable). In the second step, the impact of the selected circulation variable on the observed national hourly wind power generation (environment variable) is assessed. A detailed characterization of the circulation and environment variables are provided in Sections 3.1 and 3.2.

3.1. Atmospheric and Wind Power Data

Regarding the meteorological data, two different parameters were used according to each methodology, namely the wind speed (WS) at 10 m above ground level [10] and the mean sea level pressure (MSLP). Both parameters were obtained from the ERA-Interim Project's database [22] developed by the European Centre for Medium-Range Weather Forecasts (ECMWF) with a time

resolution of 3 h. Due to some of its specifications [22] such as: (i) the assimilation system (12-hourly 4D-Var), which provides an accurate analysis of the large-scale tropospheric circulation; and (ii) the coupling with a wave model, capable of describing the evolution of two-dimensional wave spectra at the sea surface, the Era-Interim database has been successfully applied by several authors to identify the meteorological events under analysis in this study [10,23]. The data were then selected for the time interval between January 2008 and December 2014. The area under analysis comprises the Atlantic–European region spanning from 25° N to 65° N and 60° W to 20° E, with a horizontal grid spacing of 1° × 1°.

For the purposes of this study, the methodology developed for wind power ramp detection was applied to the observed hourly aggregated wind power production series for mainland Portugal [3]. The same time interval was selected (between January 2008 and December 2014) and the data were normalized according to the wind power capacity installed at the end of each month. As described in [4], the seasonality has a major impact on wind power production, consequently, two seasons were considered: Winter (January, February, March, October, November and December) and Summer (April, May, June, July, August and September).

3.2. Cyclone and Windstorm Detection Algorithms

In this work, two algorithms for detection of critical weather situations were applied/developed to later associate the results with wind power production. Although with different applications, e.g., heavy precipitation [24] and landfalls [25], in the literature various methods [10,11,20,26] with the same purpose can be found and, despite their intrinsic characteristics, they all follow a similar structure. The first step involves the identification of the events' locations based on a determined atmospheric field, usually MSLP or WS, for each time-step. The trajectories are then obtained by connecting the events' locations between different time-steps [23].

Since low pressure systems are not always accompanied by strong winds, these will not be accounted within the windstorm detection methodologies as they are not characterized by extreme events [11]. Thus, two existing algorithms were chosen aiming the detection of certain meteorological systems: one focuses on the detection of cyclonic systems (Methodology 1) and the other is based on the detection of windstorms based on specific wind speed percentiles (Methodology 2). In the following subsections, a detailed description of both methodologies is provided.

3.2.1. Cyclone Detection Algorithm—1st Methodology

The algorithm for cyclone detection was developed at the University of Melbourne [11] and was first created for the Southern Hemisphere, having been adapted by several authors to extend its use for the Northern Hemisphere [27]. Currently, the literature related to this algorithm is abundant, and its detailed description can be found in [11,28,29].

The algorithm uses the MSLP data and identifies potential candidates through a search for a maximum in the Laplacian field for each time-step. This maximum is expected to exceed a certain user-defined threshold and, near its location, the algorithm checks for a pressure minimum. The final procedure consists in setting certain limits in order to eliminate very weak systems (<0.2 hPa (deg.lat)$^{-2}$), which can be done by smoothing the data. However, this procedure may neglect events that, despite being weak, can have some impact on the parameter under study. For this reason, a minimum intensity value, for a given radius starting in the center of the system, was considered. The threshold for the Laplacian that defines the inclusion of a system was 0.2 hPa (deg.lat)$^{-2}$ for a radius of 2 deg.lat. If the Laplacian is between 0.2 and 0.6 hPa (deg.lat)$^{-2}$, the cyclone is considered weak, if it exceeds 0.6 hPa (deg.lat)$^{-2}$, it is considered strong [28,29]. Cyclones with a life span below 6 h are also excluded from the count. The minimum distance is also analyzed for each cyclone, and only systems with a radius greater than 3 deg.lat are accounted.

The candidates are selected within a particular area, usually defined as a circle centered on the original position. All the candidates for the following position are examined and the most suitable

candidate is chosen [30]. In order to select the best candidate, a deduction for the next position is made based on the event's speed. The likelihood of the association between systems and their possible successors is determined based on a cost function [29]. This function involves the distance from the predetermined position and the pressure differential (difference between the pressure in the center of the events). The associations between the systems and their potential successors are organized by groups and, for each group, the most likely combination of associations is determined. If a system does not show any association, it means that it has just emerged (cyclogenesis) or vanished (cyclolysis). This procedure prevents the separation/junction of systems. An interesting feature of this algorithm is its ability to characterize systems as opened or closed. An opened/closed system is defined by comparing the Laplacian of the pressure field at each grid point with its neighbors [30]. When a possible low pressure is detected, the location of the pressure minimum is interpolated by using an iterative approach to the center of the ellipsoid, which best fits the surface pressure. If a closed center is not detected within a distance of 1200 km, a search is made for an opened system. The restrictions imposed on the system's strength and type enable the following classifications based on the Laplacian of the pressure field: strong closed, strong opened, weak closed and weak opened [29], which are characterised in Table 1.

Table 1. System classification based on the Laplacian of the MSLP field [29].

Class	Type	MSLP Laplacian (hPa $(\text{deg.lat})^{-2}$)
00	Strong closed	$x > 0.6$
01	Strong opened	$x > 0.6$
10	Weak closed	$0.1 < x \leq 0.6$
11	Weak opened	$0.2 < x \leq 0.6$

After running these procedures, the algorithm returns a tracking table with the different trajectories for the events and other basic characteristics, e.g., their lifetime, occurrence dates, speed, radius and its strength/type classification (strong closed, strong opened weak closed and weak opened). The algorithm was provided by the authors and it was adapted to the region of interest using the same setup as [27].

3.2.2. Windstorm Detection Algorithm—2nd Methodology

The methodology for windstorm detection was first introduced by [10]. According to the authors, the methodology starts with the determination of the grid points where the wind speed at 10 m above ground level is above a certain percentile. In this case, the 98th percentile was chosen as it is more closely related to the damages and impacts associated with such events. The 98th percentile calculation is based on the following formula [31]:

$$Perc_x = F_*^{-1}(p) = \min\{W : p \leq F_*(W)\} \quad (1)$$

where, p = 0.98 and F_* stands for the cumulative distribution function weighted by the cosine of the latitude of {W (Long, Lat, t):(Long, Lat) $\in \delta$} where δ is the domain [31]. Then, contiguous grid points for which the percentile condition occurs are enclosed into the same candidate. This step is performed using a convex hull approximation in order to identify the convex polygon containing all the points that can belong to the same synoptic event, i.e., candidate. Subsequently, the geometric center of each candidate is determined. This spatial search algorithm results in a list of the possible events associated with synoptic systems. Only events with a minimum area of 150,000 km^2 [10] are considered.

Once the synoptic events are identified, it becomes necessary to stitch to a nearest candidate at the preceding time-step to build the trajectory. In order to achieve that, some assumptions are imposed to identify the temporal sequences, such as:

1. Euclidean distance between the centers of the same event for two consecutive time-steps should not exceed a certain limit, which is set to a maximum distance of 720 km [10];
2. Only events with a minimum lifetime of 6 h and a maximum speed of 120 km/h [10] are accounted.

This procedure allows identifying whether the next event to be detected corresponds to the previously detected event or to an event that has already been recorded. All events with no continuity are eliminated, and when two or more candidates are found, a cost function is applied in order to determine the most appropriate trajectory. The cost function applied is similar to the one shown by [30], which is expressed by:

$$\text{Tracking} = \text{argmin}\left(\sum_{j=1}^{j=N}(C_t - C_{t+1,j}) \times \left(\| \frac{(Int_t - Int_{t+1,j}}{Int_t} \|\right)\right) \quad (2)$$

where, C_t are the coordinates of the center for a determined synoptic event at time step t, $C_{t+1,j}$ are the coordinates of the center for the jth synoptic event at time step $t + 1$, Int_t is the intensity observed at the geometric center of the event at time-step t and $Int_{t+1,j}$ is the intensity observed of the geometric center for the jth synoptic event at time-step $t + 1$.

As in the first methodology, the algorithm returns a tracking table with the different trajectories for the events and some basic characteristics, e.g., their lifetime, occurrence dates, speed, area of influence.

3.3. Ramp Definition

One of the biggest concerns regarding wind power management are the events usually called "wind power ramps". Currently, there is no universally accepted definition for a wind power ramp since the idea behind this concept is described as a local event, which is critical enough to deserve special attention [14]. Consequently, the characterization of these events is very difficult to achieve, since it is entirely dependent on the technical specifications of the power system in consideration [14]. According to [32], a wind power ramp occurs whenever there is a variation in energy production with considerable amplitude within a relatively short period of time. A power ramp can then be characterized by parameters [9] such as magnitude, lifetime, growth-rate, direction and occurrence time. In order to deploy a methodology capable of detecting wind power ramps, some definitions found in the literature were considered. A detailed description of these methodologies can be found in [10,33,34].

In this work, two different wind power ramp definitions (Type-1 and Type-2) were applied to the observed wind power production timeseries for the portuguese aggregate [3] as described in Section 3.1. Both definitions started with the application of a 3-h low-pass filter in the wind power data. Subsequently, the initial (i) and final (j) time-steps of a possible wind power ramp were identified based on the assumption that the derivative of power in order of time is zero:

$$Pot_{filt}(t)' = 0 \quad (3)$$

where, Pot_{filt} stands for the normalized wind power after applying the low pass filter. Additionally, this procedure allows the differentiation between downward and upward ramps. In the next step, Type-1 Ramps are evaluated. If the time between the initial and final time-steps is higher than 6 h, the standard deviation of the power series is calculated by using a moving window of 3 h. This procedure is applied for both, upward and downward ramps, and the possible wind power ramps are sorted according to the intensity of the standard deviation values. Only the 100 most intense wind power ramps were retained.

Type-2 ramps are determined based on a definition found in [9] that considers the ratio between the variation in power for two time-steps over a certain period of time and states that this ratio must be greater than a reference value PRR_{val}:

$$\frac{|Pot(t+\Delta t) - Pot(t)|}{\Delta t} \geq PRR_{val} \tag{4}$$

where Δt corresponds to 6 h. However, for this work, a PRR_{val} was not chosen, instead, the first 100 absolute ratios were considered. Having applied this methodology, the resulting upward ramps varied between 33%/6 h and 67%/6 h while resulting downward ramps varied between −35%/6 h and −56%/6 h. It should be noted that Type-1 ramps pretend to identify periods with severe variations in the wind power ramps that can have a lifetime above or equal to 6 h, while Type-2 ramps intend to detect periods with strong variations in just 6 h. Despite having different characteristics, e.g., different lifetime, the wind power ramps detected in each methodology have a non-null intersection, especially when considering extreme events, as a rapid fluctuation can occur within one other with an extended lifetime.

3.4. Evaluation of Windstorm and Cyclone Detection Methodologies

To evaluate the link between windstorms/cyclones and wind power ramps, a dichotomous approach was followed. This type of approach is usually described in a contingency table (Table 2). In this case, the evaluation process is based on the comparison between the passage of a windstorm/cyclone within an area comprised between 10° W to 5° W and 35° N to 43° N, and the time of a wind power ramp detected.

Table 2. Schematic 2 × 2 contingency table for wind power ramp detection [35].

Event Foreseen	Event Observation		Total
	Yes	No	
Yes	TP (hits)	FP (false alarms)	Foreseen Yes
No	FN (misses)	TN (true negatives)	Foreseen No
Total	Observed Yes	Observed No	N = TP + FP + FN + TN

In Table 2, TP represents the events that have been foreseen with the windstorm/cyclone detection methodologies and observed within the considered area which originated wind power ramps; FP represents the events that were foreseen within the considered area although not observed; FN represents the wind power ramp events observed that were not foreseen with the proposed methodologies; and TN represents no events foreseen/observed [36]. Different performance scores can be achieved based on the contingency table, namely the Bias Score (Bias) (5), the Extreme Dependency Score (EDS) (6), and the Hanssen & Kuipers Skill Score (KSS) (7). The EDS and KSS range between 0 and 1. The perfect classifier would have EDS = KSS = 1. The Bias ratio determines if the windstorm/cyclone detection algorithm has the tendency to over foreseen (Bias Score > 1) or under foreseen (Bias Score < 1) the number of events:

$$\text{Bias} = \frac{\text{TP} + \text{FP}}{\text{TP} + \text{FN}} \tag{5}$$

$$\text{EDS} = \frac{2\log\left(\frac{\text{TP}+\text{FN}}{N}\right)}{\log\left(\frac{\text{TP}}{N}\right)} - 1 \tag{6}$$

$$\text{KSS} = \frac{\text{TP} \times \text{TN} - \text{FP} \times \text{FN}}{(\text{TP} + \text{FN}) \times (\text{FP} + \text{TN})} \tag{7}$$

3.5. Composite Analysis

In order to verify the impact of the windstorms/cyclones on the wind power production level, a composite analysis was performed [24]. Consequently, for each point of the considered domain, it is possible to estimate the probability of a weather system to occur in combination with different levels of wind power production. Thus, and considering the entire area of each event, the probability of a certain wind power production level (Pr_{lim}) to occur, when associated with a cyclone/windstorm event (AC), is given by:

$$Pr_{lim} = \frac{AC}{TC} \tag{8}$$

where, Pr_{lim} is a certain level of wind power generation and TC stands for the total number of detected events within the given domain. Thus, for each methodology, the time-steps associated with a wind power production of more than 60% of the installed capacity and the occurrence of a cyclone/windstorm event was computed. This procedure was also carried out to identify the meteorological events related to a wind power production of less than 30% of the installed capacity. It is worth mentioning that, in order to determine the area of influence for each event, a circumference with a radius based on the average distance between the cyclone center and the edges was considered for Methodology 1 as applied in [24]. For Methodology 2, the perimeter of each candidate was obtained with the convex hull approximation.

3.6. Clustering Methodology for Trajectories Analysis

Some authors [4] highlight the close relationship between wind power ramps and the trajectories of these meteorological systems, especially in countries like Portugal, where the geographical distribution of the installed wind power capacity (with high concentration in the North/Centre regions) plays an important role in the intensity of the wind power fluctuations experienced. Hence, the knowledge behind the basic characteristics of each group of trajectories can then help in the diagnosis of the meteorological systems capable of affecting the wind power production thus, enabling preventive measures to balance the binomial production/consumption under the occurrence of wind power ramps.

Due to the great variety and diversity of trajectories obtained with both methodologies, a useful and simplistic way of analyzing the impact of such trajectories in the wind power production can consist in the aggregation of trajectories with similar characteristics. Although widely used in other different fields such as engineering, bio-informatics and marketing [34], these clustering techniques are also applied by several authors, e.g., [36–38], with the aim of classifying groups of trajectories based on similarity criteria for example cyclogenesis/cyclolysis locations, trajectory, mean intensity, among others. Thus, in order to achieve that, the K-means clustering technique was applied. This technique utilizes the Euclidean distance to split the different trajectories into K different groups, associating each trajectory to the group with the mean value closest to the sample thus, maximizing the uniformity of elements within the groups. The suitable number of K was chosen based on typical values used in literature [36] and also based on the maximum mean silhouette coefficient value. Since this technique can only be applied to trajectories with the same size, a simplistic approach to interpolate the data as described by [39] was taken. Only the events that intersect the region under analysis are considered.

4. Results and Discussion

4.1. Storm Detection

Portugal has dealt with some severe windstorms in the past, such as Gong (January 2013), Klaus (January 2009) and Xynthia (February/March 2010) [40–42]. These meteorological events are considered some of the most tragic catastrophes in the extra-tropics and are recognized for their substantial socioeconomic impacts. For instance, the windstorm Xynthia is described as the most violent since Lothar and Martin in December 1999, as it caused at least 51 deaths and 12 disappearances.

Furthermore, 2 million people lost access to electricity and more than 50,000 hectares of land have been flooded and about 10,000 people have been forced to abandon their homes on the French Atlantic Coast. Consequently, and due to the damages caused, this storm generated a total economic loss of about €3.6 billion [41]. The Xynthia storm, which crossed Western Europe between 27 February and 1 March 2010 and resulted from the development of a low pressure system to the south of the Azores Islands on 26 February 12:00 UTC [41], is here analyzed aiming to: (i) validate the Methodologies 1 and 2 and comparing the resulting trajectories to the trajectory displayed in [24,43]; (ii) prove the relationship between the passage of these meteorological phenomena and the wind power ramps in the Portuguese aggregate. Thus, in Figure 1a both the trajectories for the Methodologies 1 and 2 are presented as well as the trajectory obtained through the cyclone detection algorithm available in [43]. In Figure 1b the wind power production during the days from 26 to 28 February 2010 is also depicted.

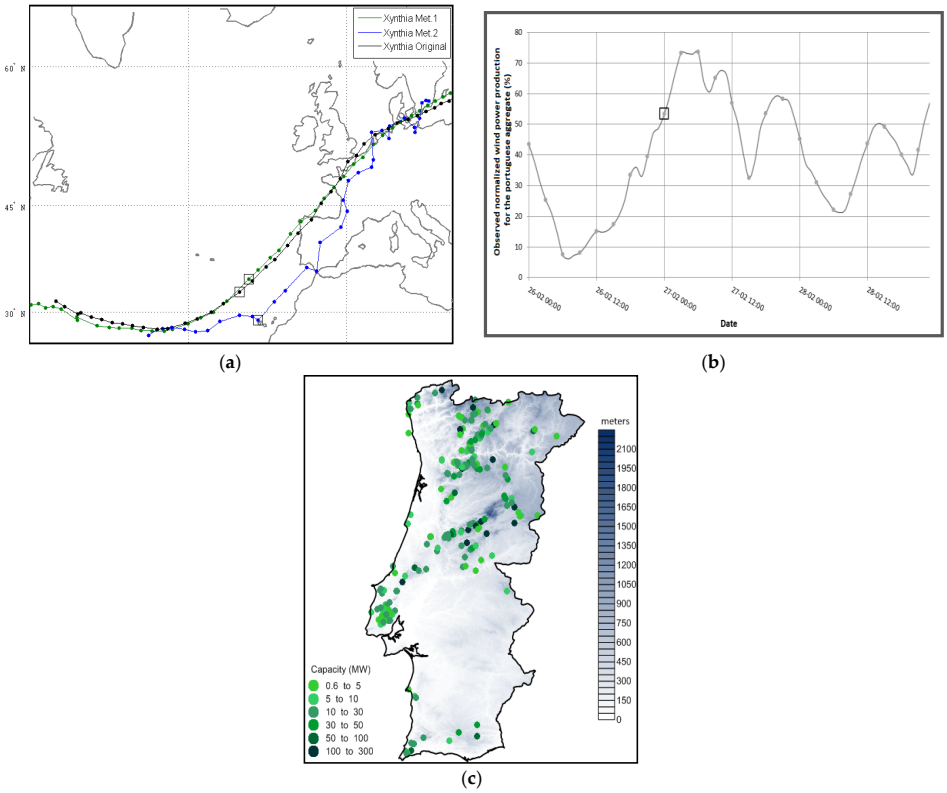

Figure 1. (**a**) Resulting trajectories for Xynthia storm with: Methodology 1 (green), Methodology 2 (blue), Original (black) [43]; (**b**) Observed normalized wind power production for the portuguese aggregate during the days 26 to 28 of February 2010. The black square marker represents the time step 27/02/2010 00:00 [3]; (**c**) Orography and wind park distribution over continental Portugal discerned by nominal power capacity [44,45].

From the analysis of Figure 1a, it is possible to easily identify a shift in trajectory when comparing both methodologies that can be explained by the definition of "center" applied for each methodology. In Methodology 2, the center of the event is defined as the geometric center of the convex hull polygon, whereas Methodology 1 searches for a minimum pressure value. Hence, when considering the rigorous definition of a low pressure system, wind speeds close to zero can be found within its center due to the absence of pressure gradients, this results in a shift towards the South when applying Methodology 2 [11]. However, both methodologies show a good agreement when comparing the resulting trajectories to the one obtained from [24,45].

Regarding the wind power production for the respective time period (Figure 1b), it is possible to verify a strong variation as the storm approaches mainland Portugal, especially when it reaches the

Azores Islands, causing the wind power production to ramp up and, as it intersects the coast near the areas where the Portuguese wind parks are concentrated (Figure 1c), the Xynthia storm causes the wind power production to ramp down at a rate of approximately 25%/3 h. Subsequently, and as the windstorm withdraws, its impact on the wind power production diminishes. These results support a close relationship between the passage of the windstorm Xynthia and the strong variations observed in the Portuguese aggregate wind power production.

4.2. Composite Analysis

Figure 2 reflects the composite analysis for Methodology 1 for both Winter and Summer months. Results suggest that there is no strong relationship between the cyclones detected and high levels of wind power production. This result can be explained by the amount of residual events detected with scarce effect on the wind power production since the criteria for event inclusion is not so strict when compared to Methodology 2, which focuses on extreme weather phenomena. For low levels of production, the results show a higher density of events during Summer months as expected, mainly explained by the Iberian thermal low [4]. As previously mentioned, Methodology 1 has the ability to categorize events in four different levels: Strong Closed (00), Strong Opened (01), Weak Closed (10) and Weak Opened (11), hence, these four categories were analyzed in order to determine which are the most related to high levels of wind power production for Winter.

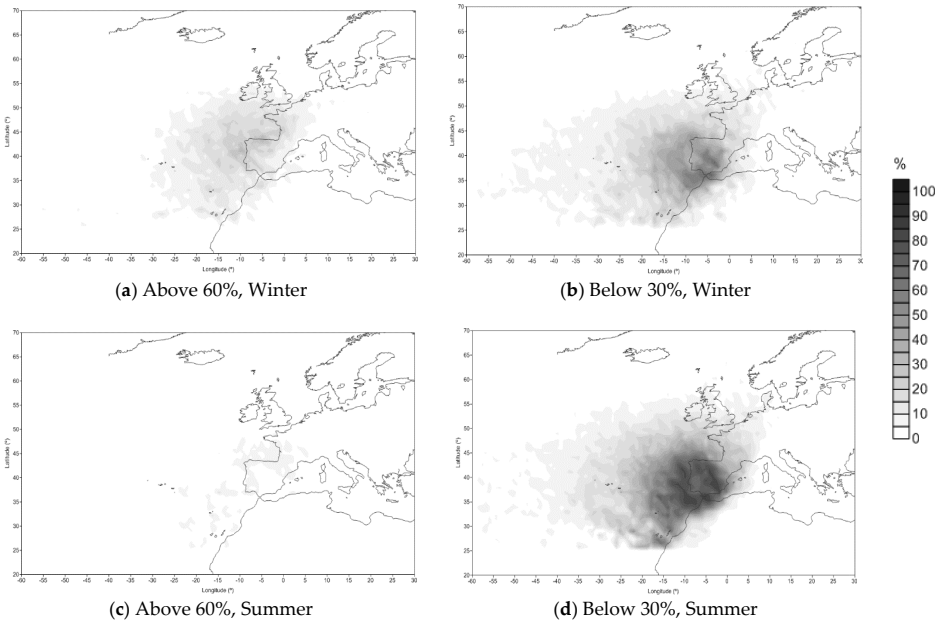

(**a**) Above 60%, Winter (**b**) Below 30%, Winter

(**c**) Above 60%, Summer (**d**) Below 30%, Summer

Figure 2. Composite analysis for Methodology 1 for all events with a production (**a**) higher than 60% of the installed capacity for Winter (**b**) lower than 30% of the installed capacity for Winter (**c**) higher than 60% of the installed capacity for Summer (**d**) lower than 30% of the installed capacity for Summer. The TC values are 364 and 384 for the Winter and Summer period, respectively.

Thus, the composite analysis for these events was only carried out for power production levels higher than 60% of the installed capacity, Figure 3. From Figure 3, it is clear that 00 and 01 events are the ones with the highest impact on the wind power production. It is also possible to identify the main differences between closed and opened events regarding their spatial distribution and level of impact, as the first ones are perfectly identifiable with specific locations and high density regions (mostly located near the Northwestern region of the Iberian Peninsula), whereas opened events tend to show a more dispersed distribution. Further details regarding the impact of each class, namely the

TC values and respective frequency of occurrence, for each class during the Winter season is provided in Table 3.

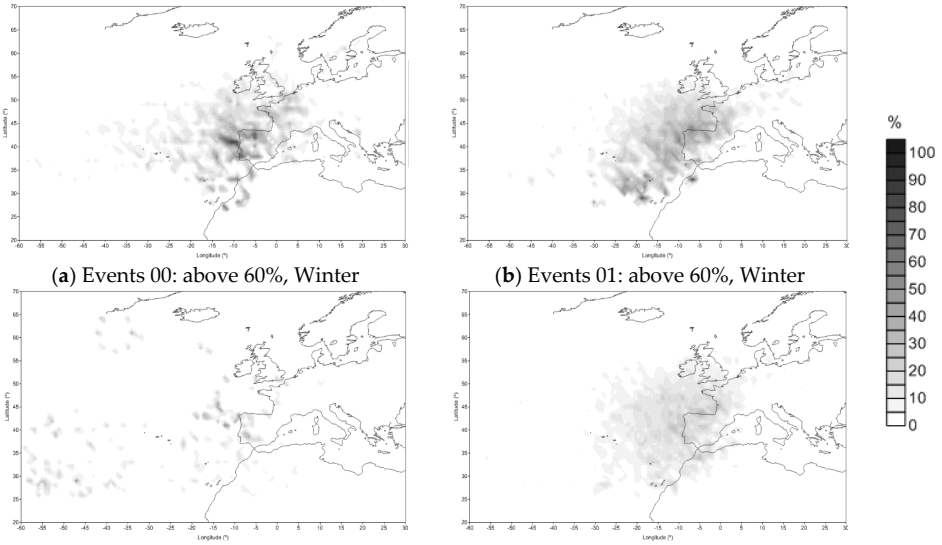

(**a**) Events 00: above 60%, Winter (**b**) Events 01: above 60%, Winter

(**b**) Events 10: above 60%, Winter (**d**) Events 11: above 60%, Winter

Figure 3. Composite analysis for Methodology 1 for Winter months with a power production higher than 60% over the installed capacity: (**a**) 00 events; (**b**) 01 events; (**c**) 10 events; (**d**) 11 events. The TC values are 36, 73, 50 and 205 for Events 00, 01, 10 and 11, respectively.

Table 3. *TC* values and frequency of occurrence (%) for each class of event identified in Met. 1 for Winter months.

Class	TC	Frequency of Occurrence (%)
00	36	9.89
01	73	20.05
10	50	13.74
11	205	56.32

From Table 3, it is possible to depict that the most common events are, as expected, weak opened events (11). Based on the previous results, weak opened events are associated with low levels of wind power production in Portugal. Considering the strong events (00 and 01), the most common are, as well, opened ones. Therefore, despite the reduced frequency of occurrence of strong closed events (00), the tendency is for these events to be associated with high levels of wind power production.

The composite analysis was also performed for Methodology 2. Thus, in Figure 4 the composite analysis for both Winter and Summer months in cases where the power production is higher than 60% and lower than 30% of the installed capacity are shown. From Figure 4 it is clear that the events, which intersect Continental Portugal in the Northern/Centre regions, are more related to higher levels of wind production during the Winter. On the other hand, low levels of wind power production are associated with the occurrence of windstorm events in the South region of Portugal (Figure 4b). This result can be explained by the condensed installed wind power capacity over the Centre/Northern regions of Portugal [4]. In the summer, the meteorological events associated with higher levels of power production are mostly originated within the Iberian Peninsula, due to the presence of the Iberian thermal low.

Based on the previous results, it is possible to conclude that: (i) the events with most impact on the wind power production are the ones that intersect the Northern/Centre region of Portugal; (ii) for Methodology 1 the Strong Closed (00) and Strong Opened (01) events are the ones with the greatest impact, although their spatial distribution shows different features; (iii) the cyclone detection methodology presents more difficulties in highlighting regions with higher probability of occurrence,

especially for wind power production levels above 60%; and (iv) Methodology 2 is well representative of the regions with the greatest impact due to intrinsic characteristics associated with the strength of the detected events. The previous results highlighted the association between the windstorms/cyclones and different levels of wind power production.

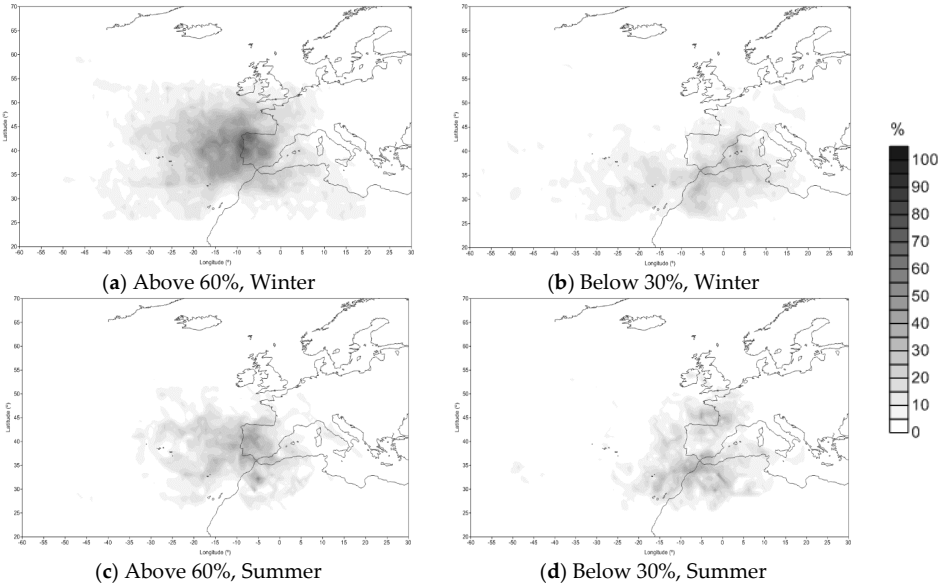

(**a**) Above 60%, Winter (**b**) Below 30%, Winter

(**c**) Above 60%, Summer (**d**) Below 30%, Summer

Figure 4. Composite analysis for Methodology 2 for all events with a production (**a**) higher than 60% over the installed capacity for Winter (**b**) lower than 30% over the installed capacity for Winter (**c**) higher than 60% over the installed capacity for Summer (**d**) lower than 30% over the installed capacity for Summer. The TC values are 151 and 91 for Winter and Summer months, respectively.

4.3. Evaluation of Proposed Methodologies

The results above suggest a relationship between wind power production and large-scale meteorological systems. Thus, in order to complement this analysis and to prove the applicability of such methodologies in the detection of wind power ramps, a validation based on the dichotomous evaluation metrics was carried out for both Winter and Summer seasons. The contingency tables used to determine the evaluation metrics are presented below (Tables 4–7).

The evaluation metrics chosen for this purpose were the Bias Score, the KSS Score and the EDS Score for which the results are shown in Figure 5. It is worth mentioning that both upward and downward ramps (Type-1 and Type-2) were analyzed.

From the analysis of Figure 5, it is possible to verify the tendency for Methodology 1 to overestimate (Bias Score significantly higher than 1) the number of detected events which, as explained above, can be associated to the low threshold imposed to the intensity of each candidate, resulting in a considerable higher amount of false alarms in comparison to Methodology 2. This result is even more prominent during the Summer as the atmospheric conditions promote the cyclogenesis over the Iberian Peninsula, namely due to the presence of the Iberian thermal low that, although with some impact on the wind power production, it is not commonly associated with wind power ramps. The EDS Score shows similar results for both methodologies with the highest values scored in Methodology 2 for Type-1 downward ramps, especially during the Summer. Regarding the KSS Score, the best score was obtained with Methodology 2 during the Summer, favoring a higher capacity to distinguish events that effectively caused a wind power ramp from the remaining ones in comparison to Methodology 1. Overall, and based on the performance obtained with the different metrics, the Methodology 2 shows a higher capability to detect severe wind power ramps.

Table 4. Contingency table for upward ramps detected with Methodologies 1 and 2 for Winter.

Event Foreseen	Event Observation								Total			
	Yes				No							
	Type-1 Met.1	Type-1 Met.2	Type-2 Met.1	Type-2 Met.2	Type-1 Met.1	Type-1 Met.2	Type-2 Met.1	Type-2 Met.2	Type-1 Met.1	Type-1 Met.2	Type-2 Met.1	Type-2 Met.2
Yes	59	60	56	46	305	91	308	105	364	151	364	151
No	22	21	22	32	9822	10,036	9822	10,025	9844	10,057	9844	10,057
Total	81	81	78	78	10,127	10,127	10,130	10,130	10,208	10,208	10,208	10,208

Table 5. Contingency table for downward ramps detected with Methodologies 1 and 2 for Winter.

Event Foreseen	Event Observation								Total			
	Yes				No							
	Type-1 Met.1	Type-1 Met.2	Type-2 Met.1	Type-2 Met.2	Type-1 Met.1	Type-1 Met.2	Type-2 Met.1	Type-2 Met.2	Type-1 Met.1	Type-1 Met.2	Type-2 Met.1	Type-2 Met.2
Yes	60	55	44	39	304	96	320	112	364	151	364	151
No	19	24	28	33	9825	10,033	9816	10,024	9844	10,057	9844	10,057
Total	79	79	72	72	10,129	10,129	10,136	10,136	10,208	10,208	10,208	10,208

Table 6. Contingency table for upward ramps detected with Methodologies 1 and 2 for Summer.

Event Foreseen	Event Observation								Total			
	Yes				No							
	Type-1 Met.1	Type-1 Met.2	Type-2 Met.1	Type-2 Met.2	Type-1 Met.1	Type-1 Met.2	Type-2 Met.1	Type-2 Met.2	Type-1 Met.1	Type-1 Met.2	Type-2 Met.1	Type-2 Met.2
Yes	12	16	16	16	372	75	368	75	384	91	384	91
No	7	3	6	6	9857	10,154	9858	10,151	9864	10,157	9864	10,157
Total	19	19	22	22	10,229	10,229	10,226	10,226	10,248	10,248	10,248	10,248

Table 7. Contingency table for downward ramps detected with Methodologies 1 and 2 for Summer.

Event Foreseen	Event Observation								Total			
	Yes				No							
	Type-1 Met.1	Type-1 Met.2	Type-2 Met.1	Type-2 Met.2	Type-1 Met.1	Type-1 Met.2	Type-2 Met.1	Type-2 Met.2	Type-1 Met.1	Type-1 Met.2	Type-2 Met.1	Type-2 Met.2
Yes	17	19	21	16	367	72	363	75	384	91	384	91
No	4	2	7	12	9860	10,155	9857	10,145	9864	10,157	9864	10,157
Total	21	21	28	28	10,227	10,227	10,220	10,323	10,248	10,248	10,248	10,248

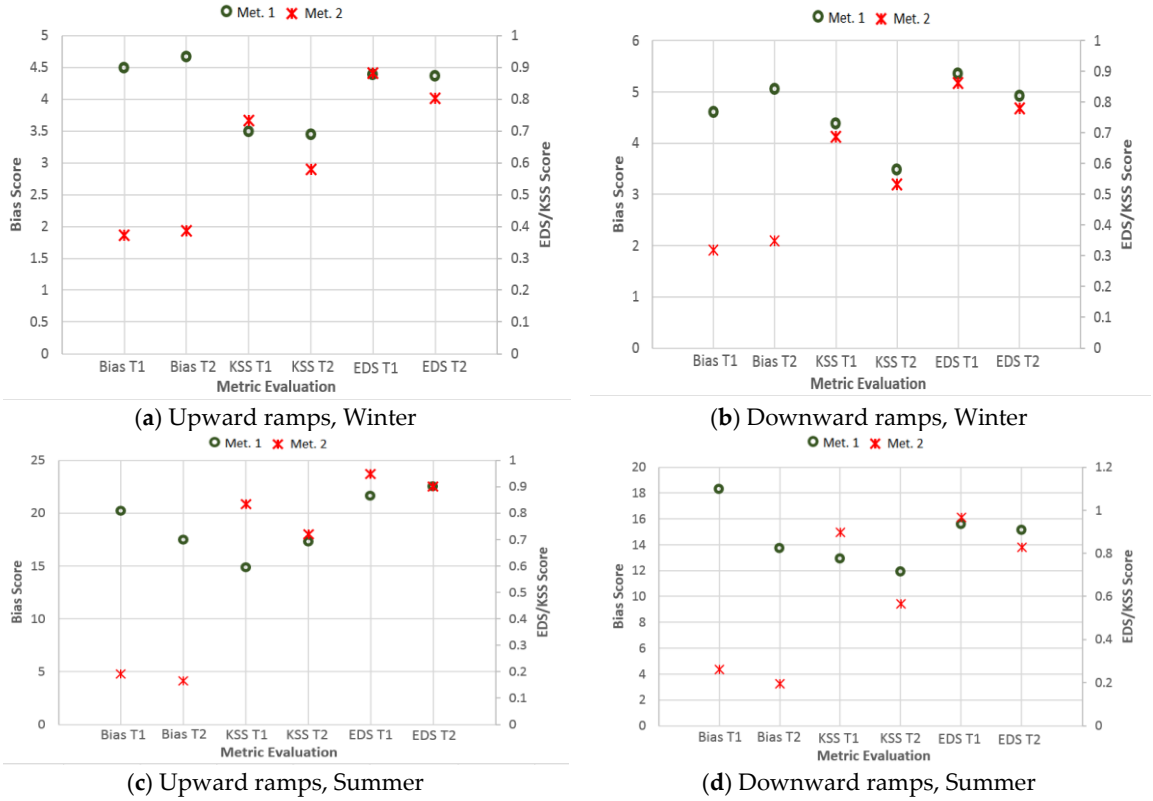

(**a**) Upward ramps, Winter

(**b**) Downward ramps, Winter

(**c**) Upward ramps, Summer

(**d**) Downward ramps, Summer

Figure 5. Evaluation metrics for: (**a**) Upward ramps during Winter months; (**b**) Downward ramps during Winter months; (**c**) Upward ramps during Summer months; (**d**) Downward ramps during Summer months.

4.4. Trajectories Analysis

In order to gain further insights regarding the windstorms/cyclones features and their impact on wind power ramps, an analysis of the common trajectories of these events was performed using a K-means methodology. Hence, the K-means clustering technique was applied with K = 6 (Figure 6). Some key parameters associated with wind power ramps were chosen to better characterize the clusters. Therefore, and for the lifetime of each windstorm/cyclone, the following parameters were obtained and grouped by the corresponding cluster: average wind power production during the occurrence of the events, the maximum/minimum derivative of the power production in order of time (in intervals of 6 h), standard deviation of the wind power production, propagation speed and the duration of the event. The last two parameters intend to provide more details regarding the meteorological features of each cluster allowing a proper accommodation of the impact caused by the detected events on the power system, while the remaining parameters allow the understanding of the impact caused by each type of event in the observed wind power production. The results are presented in box-and-whiskers plots where the median is drawn in red and the edges of the box are the 25th and 75th percentiles and the whiskers extend to 1.57 times the interquartile range of the box edges (Figures 7 and 8). The outliers are marked by a red cross and represent the values outside the whisker length. This analysis is only shown for the winter months since, as previously discussed, during the summer months local phenomena promote the cyclogenesis and cyclolysis over the Iberian Peninsula. Additionally, the events with the highest impact on the wind power production occur during the winter months [4].

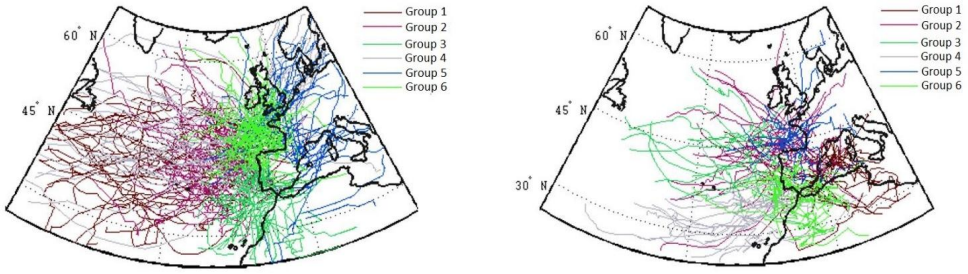

(**a**) Met.1, Winter (**b**) Met. 2, Winter

Figure 6. Groups of trajectories based on the K-means clustering with K equal 6 for Winter months: (**a**) Methodology 1; (**b**) Methodology 2.

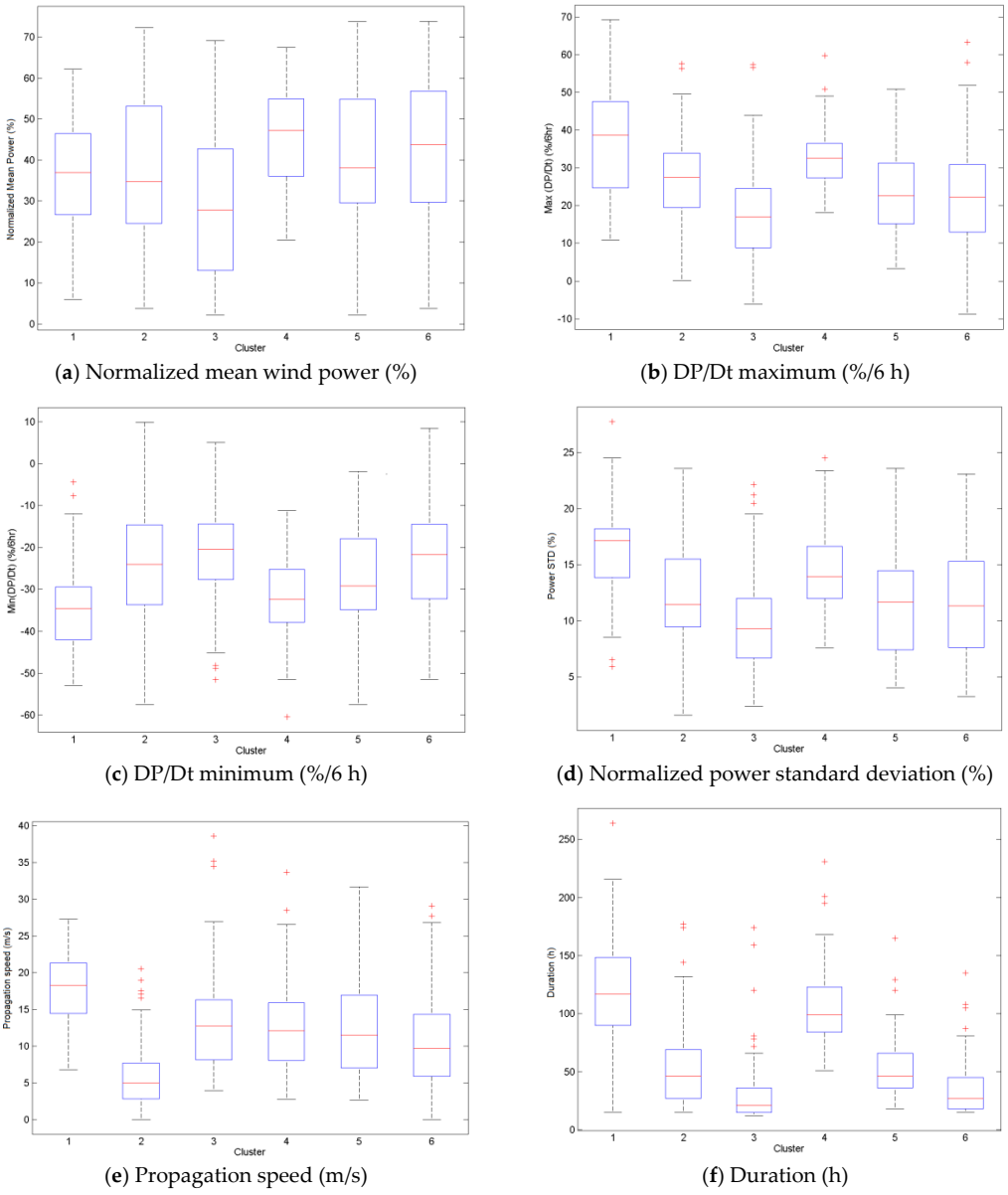

(**a**) Normalized mean wind power (%) (**b**) DP/Dt maximum (%/6 h)

(**c**) DP/Dt minimum (%/6 h) (**d**) Normalized power standard deviation (%)

(**e**) Propagation speed (m/s) (**f**) Duration (h)

Figure 7. Main characteristics of the different trajectories clusters and their impact in the wind power production—Methodology 1.

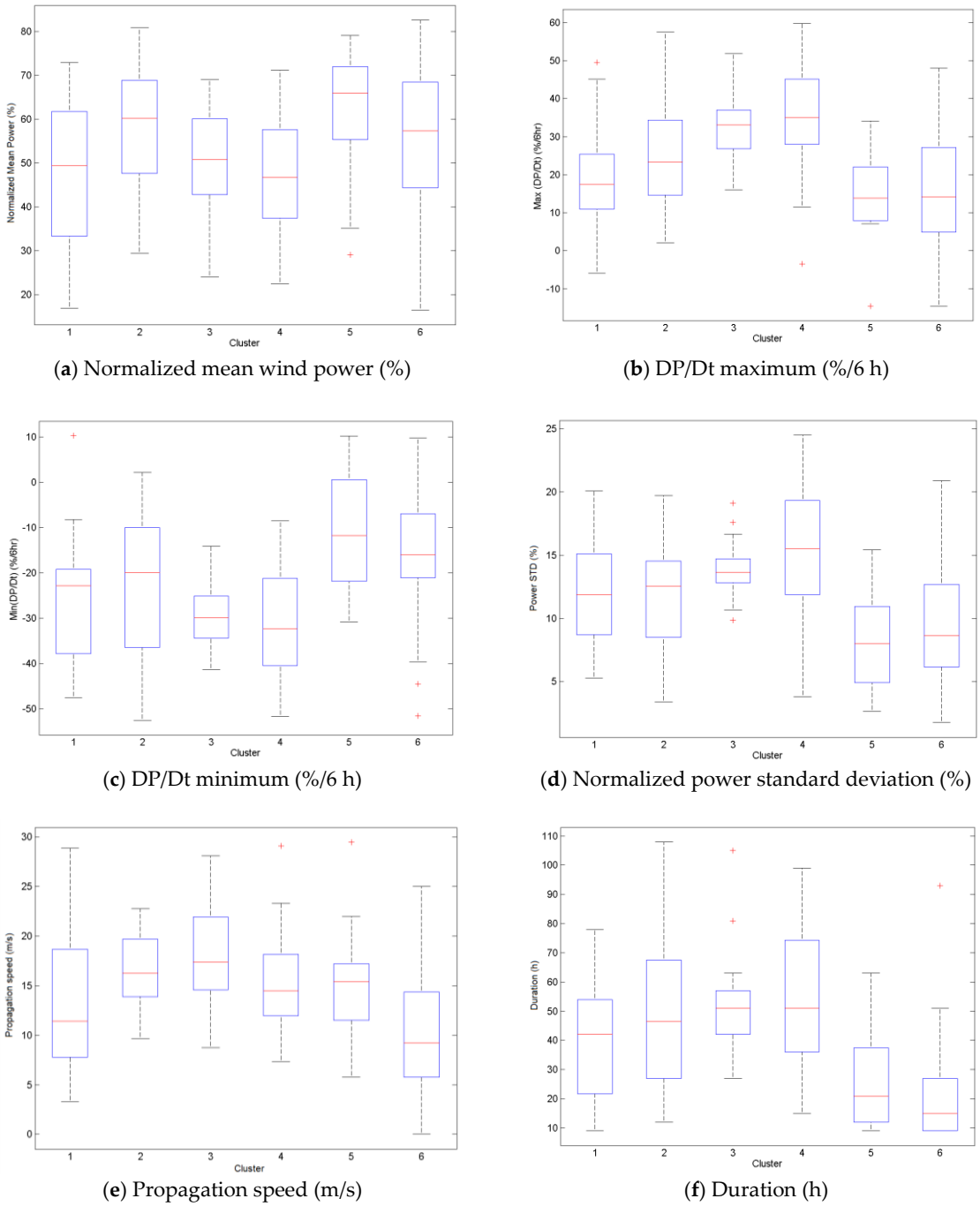

Figure 8. Main characteristics of the different trajectories clusters and their impact in the wind power production—Methodology 2.

From Figure 6, it is possible to verify the difference regarding the number of detected events, with Methodology 1 showing high density clusters in comparison to Methodology 2. Additionally, in the case of Methodology 2, it is possible to identify a more distinct zone of influence of each group. Notwithstanding, the Methodology 1 tends to present trajectories with a lifetime higher than the Methodology 2 allowing to monitor in an early stage, and consequently, it is possible a better accommodation of these phenomena in the management of the power system.

For Methodology 1 (Figure 7), the results show that the group with the highest normalized mean power is group 4. Regarding the power derivatives in order of time, both the maximum and the

minimum are observed in the group 1. The maximum normalized power standard deviation was also obtained for group 1. Thus, it is possible to verify that the group with the greatest impact on the variability of wind power production over Continental Portugal is group 1, which intersects the coast from the Western/Southwestern regions. On the other hand, group 3, which predominates the southern region of the Iberian Peninsula, shows the lowest impact regarding the wind power variability. The lowest duration events are expected in group 3, while group 1 presents the highest average duration and propagation speed. These results support the geographical extension of this group shown in Figure 6a, suggesting that the majority of its events have their cyclogenesis far away from the coast, however, as the events approach the continent, their impact on the wind power production is more evident. Thus, these cyclone peculiarities are highly relevant for the TSO as, according to their average duration, they can be monitored long before some significant impact on the wind power production can be detected, allowing to properly accommodate the impact of such events into the power system. Group 2 presents the lower propagation speed values observed. Consequently, this result can partly explain the high normalized mean power values, which are not associated with strong wind power variability, i.e., with the slow upcoming of cyclones the wind power production tends to increase smoothly.

From Figure 8, it can be seen that the group with the highest normalized mean power is group 5. Nevertheless, this cluster shows a reduced impact regarding the parameters associated with wind power variability. This group is essentially located in the North region of the Iberian Peninsula. Group 6, located at South of Portugal, also shows a reduced impact in the critical parameters associated to wind power ramps. However, the group with the highest maximum derivative of the normalized power in order of time is group 4, which also shows the (i) minimum derivative of the normalized power in order of time and (ii) the greatest standard deviation of the wind power production. This result classifies group 4 as the group with the greatest impact on the wind power production leading to a possible occurrence of severe variations in the Portuguese wind power production. This group is originated in the Southwestern region of the Iberian Peninsula and moves, mostly, towards the Iberian Peninsula coast, with a high number of events intersecting the coast of mainland Portugal. As in Methodology 1, this group is also the one with the highest duration, which implies a higher extension in comparison to the other groups. However, and as previously mentioned, its average duration is much lower than the one presented with the latter, which suggests that a combination of both methodologies needs to be considered, as the first has the ability of detecting the event long before its major impacts on wind power production are detected, and the latter has the ability of determining the time when the event reaches its peak. Group 3 shows the highest propagation speed, and together with Group 4, the two groups are the ones mostly associated with strong wind power variability. Therefore, in both methodologies, the results suggest that the propagation speed is an important windstorm/cyclone characteristic. On the other hand, the duration of the event shows a reduced impact on the observed wind power production variability.

When comparing the clusters for both methodologies and considering their geographical location and intrinsic characteristics, the easterly clusters are the ones with more similarities, aside from their duration and propagation speed (which can be explained by the short lifetime of the windstorms detected in Methodology 2). Despite the ability of Methodology 1 to detect the full trajectory of the meteorological systems, Methodology 2 provides a more clear and specific location of the zones with critical impact on the wind power production. This last aspect can be easily observed on Figure 6a where it is possible to depict a large dispersion in the trajectories held by groups 1, 2 and 4. Additionally, it is also possible to verify that the propagation speed parameter is a good index concerning the variability of the wind power production for Methodology 1, however, this fact is not so evident for Methodology 2.

5. Conclusions

In this paper, two different methodologies were applied to identify the impact of critical weather situations in the wind power generation, namely during the so-called "wind power ramp events". Methodology 1 is based on a cyclone detection algorithm, while Methodology 2 is based on the detection of windstorms.

The windstorm detection algorithm shows a higher performance concerning the identification of wind power ramps when compared with the cyclone detection algorithm since Methodology 1 tends to overestimate the number of wind power ramp events. With this study, it was possible to identify some key features (e.g., trajectories) from the meteorological structures that unleash wind power ramps. Severe variations in the Portuguese wind power production are mainly associated with the cyclones and windstorms originated in the Southwestern region of the Iberian Peninsula. On the other hand, events with trajectories in the North of the Iberian Peninsula tend to produce a high level of wind power production, but are not associated with large wind power ramps. Such information can be very useful to the TSOs, as it can help in the decision making process by complementing the actual existing wind power forecast tools, thus enabling the adoption of preventive measures to ensure the stability of the power system, e.g., by committing additional reserves or activating special frequency control modes for the operation of wind turbines.

As future work, a more detailed analysis on the impact of each type of class from Methodology 1 on the wind power production, specially under the occurrence of wind power ramps, is to be carried out. Additionally, to mitigate the possible impact induced by the use of surface wind speed, the Methodology 2 will be applied to wind speed data extracted near the typical wind turbine hub height.

Acknowledgments: This work was supported by the Integrated Research Programme on Wind Energy (IRPWIND), Grant agreement number: 609795. The authors gratefully acknowledge Kevin Keay and Ian Simmonds at the University of Melbourne for providing the cyclone detection algorithm, and Tiago Rodrigues for providing the setup of this algorithm for the Northern Hemisphere.

Author Contributions: M.L., A.C. and A.E. conceived and designed the methodologies; M.L. performed the experiments; M.L., A.C. and A.E. analyzed the data and wrote the paper.

Conflicts of Interest: The authors declare no conflict of interest.

References

1. Estanqueiro, A. Impact of Wind Generation Fluctuations in the Design and Operation of Power Systems. In Proceedings of the 7th international Workshop on Large Scale Integration of Wind Power and on Transmission Networks for Offshore Wind Farms, Madrid, Spain, 26–27 May 2008; p. 7.
2. Marquis, M.; Wilczak, J.; Ahlstrom, M.; Sharp, J.; Stern, A.; Smith, J.C.; Calvert, S. Forecasting the Wind to Reach Significant Penetration Levels of Wind Energy. *Bull. Am. Meteorol. Soc.* **2011**, *92*, 1159–1171. [CrossRef]
3. REN—Centro de Informação. Available online: http://www.centrodeinformacao.ren.pt/EN/Pages/CIHomePage.aspx (accessed on 10 January 2016).
4. Couto, A.; Costa, P.; Rodrigues, L.; Lopes, V.; Estanqueiro, A. Impact of Weather Regimes on the Wind Power Ramp Forecast in Portugal. *IEEE Trans. Sustain. Energy* **2015**, *6*, 934–942. [CrossRef]
5. Bessa, R.J.; Matos, M.A.; Costa, I.C.; Bremermann, L.; Franchin, I.G.; Pestana, R.; Machado, N.; Waldl, H.; Wichmann, C. Reserve setting and steady-state security assessment using wind power uncertainty forecast: A case study. *IEEE Trans. Sustain. Energy* **2012**, *3*, 827–836. [CrossRef]
6. Bessa, R.J.; Moreira, C.; Silva, B.; Matos, M. Handling renewable energy variability and uncertainty in power systems operation. *Wiley Interdiscip. Rev. Energy Environ.* **2014**, *3*, 156–178. [CrossRef]
7. Potter, C.W.; Grimit, E.; Nijssen, B. Potential benefits of a dedicated probabilistic rapid ramp event forecast tool. In Proceedings of the 2009. PSCE '09. IEEE/PES Power Systems Conference and Exposition, Seattle, WA, USA, 15–18 March 2009; p. 5.
8. Steiner, A.; Köhler, C.; Metzinger, I.; Braun, A.; Zirkelbach, M.; Ernst, D.; Tran, P.; Ritter, B. Critical weather situations for renewable energies—Part A:Cyclone detection for wind power. *Renew. Energy* **2017**, *101*, 41–50. [CrossRef]

9. Ouyang, T.; Zha, X.; Qin, L. A Survey of Wind Power Ramp Forecasting. *Energy Power Eng.* **2013**, *5*, 368–372. [CrossRef]
10. Renggli, D. Seasonal Predictability of Wintertime Windstorm Climate Over the North Atlantic and Europe. Ph.D. Thesis, Freien Universitat Berlin, Berlin, Germany, 2011.
11. Murray, R.J.; Simmonds, I. A Numerical Scheme for Tracking Cyclone Centres From Digital Data. Part I: Development and Operation of the Scheme. *Aust. Meteorol. Mag.* **1991**, *39*, 155–166.
12. Cutler, N. Characterising the Uncertainty in Potential Large Rapid Changes in Wind Power Generation. Ph.D. Thesis, University of New South Wales, Sydney, Australia, 2009.
13. Holttinen, H.; Milligan, M.; Ela, E.; Menemenlis, N.; Dobschinski, J.; Rawn, B.; Bessa, R.J.; Flynn, D.; Gomez-Lazaro, E.; Detlefsen, N.K. Methodologies to Determine Operating Reserves due to Increased Wind Power. *IEEE Trans. Sustain. Energy* **2012**, *3*, 713–723. [CrossRef]
14. Gallego-Castillo, C.; Cuerva-Tejero, A.; Lopez-Garcia, O. A Review on the Recent History of Wind Power Ramp Forecasting. *Renew. Sustain. Energy Rev.* **2015**, *52*, 1148–1157. [CrossRef]
15. Walton, R.A.; Gallus, W.A.; Takle, E.S. Wind Ramp Events at Turbine Height-Spatial Consistency and Causes at two Iowa Wind Farms. In Proceedings of the Fourth Conference Weather, Climate, New Energy Economy, Austin, TX, USA, 5 January 2013; p. 7.
16. Zack, J.W. Optimization of Wind Power Production Forecast Performance During Critical Periods for Grid Management. In Proceedings of the European Wind Energy Conference EWEC, Milano, Italy, 7–10 May 2007.
17. Musilek, P. Forecasting of Wind Ramp Events—Analysis of Cold Front Detection. In Proceedings of the 31th International Symposium on Forecasting, Prague, Czech Republic, 26–29 June 2011.
18. Freedman, J.; Markus, M.; Penc, R. Analysis of West Texas Wind Plant Ramp-Up and Ramp-Down Events. 2008. Available online: http://interchange.puc.state.tx.us/WebApp/Interchange/Documents/33672_1014_580034.PDF (accessed on 15 March 2017).
19. Walton, R.A.S. Analysis of Ramp Events and Two-Day Persistent Forecast Accuracy at 80m. In Proceedings of the Research Experiences for Undergraduates—Symposium; 2012. Available online: http://www.meteor.iastate.edu/windresearch/resources/Binder1.pdf (accessed on 16 October 2016).
20. Li, Y.; Musilek, P.; Lozowski, E. Identification of Atmospheric Pressure Troughs using Image Processing Techniques. In Proceedings of the 2013 Joint IFSA World Congress NAFIPS Annual Meeting (IFSA/NAFIPS), Edmonton, AB, Canada, 24–28 June 2013; pp. 722–726.
21. Huth, R.; Beck, C.; Philipp, A.; Demuzere, M.; Ustrnul, Z.; Tveito, O.E. Classifications of Atmospheric Circulation Patterns Recent Advances and Applications. *Trends Dir. Clim. Res.* **2008**, *1146*, 105–152.
22. Dee, D.P.; Uppala, S.M.; Simmons, A.J.; Berrisford, P.; Poli, P.; Kobayashi, S.; Andrae, U.; Balmaseda, M.A.; Balsamo, G.; Bauer, P.; et al. The ERA-Interim reanalysis: Configuration and performance of the data assimilation system. *Q. J. R. Meteorol. Soc.* **2011**, *137*, 553–597. [CrossRef]
23. Roberts, J.F.; Champion, A.J.; Dawkins, L.C.; Hodges, K.I.; Shaffrey, L.C.; Stephenson, D.B.; Stringer, M.A.; Thornton, H.E.; Youngman, B.D. The XWS open access catalogue of extreme European windstorms from 1979 to 2012. *Nat. Hazards Earth Syst. Sci.* **2014**, *14*, 2487–2501. [CrossRef]
24. Iordanidou, V.; Koutroulis, A.G.; Tsanis, I.K. A Probabilistic Rain Diagnostic Model Based on Cyclone Statistical Analysis. *Adv. Meteorol.* **2014**, *2014*. [CrossRef]
25. Zhang, W.; Leung, Y.; Wang, Y. Cluster Analysis of Post-Landfall Tracks of Landfalling Tropical Cyclones Over China. *Clim. Dyn.* **2013**, *40*, 1237–1255. [CrossRef]
26. Bosler, P.A.; Roesler, E.L.; Taylor, M.A.; Mundt, M. Stride Search: a general algorithm for storm detection in high resolution climate data. *Geosci. Model Dev. Discuss.* **2015**, *8*, 7727–7765. [CrossRef]
27. Rodrigues, T.F.C. Ciclones No Oceano Atlântico Norte—Clima Atual e Cenário Futuro. Master's Thesis, Universidade de Aveiro, Aveiro, Portugal, 2011.
28. Murray, R.J.; Simmonds, I. A Numerical Scheme for Tracking Cyclone Centres From Digital Data. Part II: Application to January and July General Circulation Model Simulations. *Aust. Meteorol. Mag.* **1991**, *39*, 167–180.
29. Pinto, J.G.; Spangehl, T.; Ulbrich, U.; Speth, P. Sensitivities of a Cyclone Detection and Tracking Algorithm: Individual Tracks and Climatology. *Meteorol. Z.* **2005**, *14*, 823–838. [CrossRef]
30. Flaounas, E.; Kotroni, V.; Lagouvardos, K.; Flaounas, I. Tracking Winter Extra-Tropical Cyclones Cased on Their Relative Vorticity Evolution and Sensitivity to Prior Data Filtering (cycloTRACK v1.0). *Geosci. Model Dev. Discuss.* **2014**, *7*, 1245–1276. [CrossRef]

31. Hannachi, A.; Jolliffe, I.T.; Stephenson, D.B. The Return Period of Wind Storms Over Europe. *Int. J. Climatol.* **2008**, *29*, 437–459.
32. Truewind, A. AWS Truewind's Final Report for the Alberta Forecasting Pilot Project. *Wind Power Forecasting PILOT Project.* **2008**, 66.
33. Davy, R.J.; Woods, M.J.; Russell, C.J.; Coppin, P.A. Statistical Downscaling of Wind Variability From Meteorological Fields. *Bound.-Layer Meteorol.* **2010**, *135*, 161–175. [CrossRef]
34. Peters, G.; Crespo, F.; Lingras, P.; Weber, R. Soft clustering—Fuzzy and Rough Approaches and Their Extensions and Derivatives. *Int. J. Approx. Reason.* **2013**, *54*, 307–322. [CrossRef]
35. Ferreira, C.; Gama, J.; Matias, L.; Botterud, A.; Wang, J. *A Survey on wind Power Ramp Forecasting*; Technical Report; Argonne National Laboratory (ANL): Lemont, IL, USA, 2011.
36. Gaffney, S.J.; Robertson, A.W.; Smyth, P.; Camargo, S.J.; Ghil, M. Probabilistic clustering of extratropical cyclones using regression mixture models. *Clim. Dyn.* **2007**, *29*, 423–440. [CrossRef]
37. Ramsay, H.A.; Camargo, S.J.; Kim, D. Cluster Analysis of Tropical Cyclone Tracks in the Southern Hemisphere. *Clim. Dyn.* **2012**, *39*, 897–917. [CrossRef]
38. Camargo, S.J.; Robertson, A.W.; Gaffney, S.J.; Smyth, P.; Ghil, M. Cluster analysis of typhoon tracks. Part I. General properties. *J. Clim.* **2007**, *20*, 3635–3653. [CrossRef]
39. Kim, H.-S.; Kim, J.-H.; Ho, C.-H.; Chu, P.-S. Pattern Classification of Typhoon Tracks Using the Fuzzy c-Means Clustering Method. *J. Clim.* **2011**, *24*, 488–508. [CrossRef]
40. Liberato, M.L.R. The 19 January 2013 Windstorm Over the North Atlantic: Large-Scale Dynamics and Impacts on Iberia. *Weather Clim. Extrem.* **2014**, *5–6*, 16–28. [CrossRef]
41. Nerushev, A.F.; Barkhatov, A.E.; Region, K. Determination of Atmospheric Characteristics in the Zone of Action of Extra-Tropical Cyclone Xynthia (February 2010) Inferred from Satellite Measurement Data. In Proceedings of the 2012 EUMETSAT Meteorological Satellite Conference, Sopot, Poland, 3–7 September 2012.
42. EUmetrain. Available online: http://www.eumetrain.org/resources/the_xynthia_storm_by_ascat_2012.html (accessed on 5 January 2016).
43. Extreme Wind Storms Catalogue. Available online: http://www.europeanwindstorms.org/ (accessed on 24 April 2017).
44. Aster, G.; Validation Team. *ASTER Global Digital Elevation Model Version 2—Summary of Validation Results*; NASA: Washington, DC, USA, 2011.
45. Portal e2p. Available online: http://e2p.inegi.up.pt/ (accessed on 20 November 2016).